



Cross-linked gel polymer electrolyte containing multi-wall carbon nanotubes for application in dye-sensitized solar cells

João E. Benedetti, Aline A. Corrêa, Mayara Carmello, Luiz C.P. Almeida, Agnaldo S. Gonçalves, Ana F. Nogueira*

Institute of Chemistry, University of Campinas – UNICAMP, P.O. Box 6154, 13083-970, Campinas, SP, Brazil

ARTICLE INFO

Article history:

Received 18 November 2011
Received in revised form 26 January 2012
Accepted 27 January 2012
Available online 19 February 2012

Keywords:

Gel polymer electrolyte
Multi-wall carbon nanotube
Dye sensitized solar cells

ABSTRACT

A cross-linked gel polymer electrolyte composed of poly (ethylene oxide-co-2-(2-methoxyethoxy) ethyl glycidyl ether-co-allyl glycidyl ether, γ -butyrolactone, LiI and I₂, mixed with functionalized multi-wall carbon nanotubes (MWCNT), was applied in dye-sensitized solar cells (DSSC). The electrolyte was characterized by differential scanning calorimetry, conductivity measurements and Raman spectroscopy. Due to its nature, the terpolymer was chemically cross-linked during DSSC assembly to give rise to quasi-solid state solar cells. The gel polymer electrolyte containing 1 wt% of MWCNT exhibited conductivity values higher than 10^{-3} S cm⁻¹. An increase in MWCNT content provided a smaller concentration of polyiodide species, as confirmed by Raman spectroscopy. The highest photocurrent (8.74 mA cm⁻²) was achieved by DSSC based on the cross-linked gel polymer electrolyte containing 1 wt% of MWCNT compared to DSSC based on non-cross-linked gel polymer electrolytes (7.93 mA cm⁻²). The incorporation of 3 wt% of MWCNT into the gel polymer electrolyte promoted a decrease in both J_{sc} and V_{oc} , probably due to poorer light transmittance of the electrolyte in the visible range and higher charge recombination losses, respectively. Thus, the highest efficiency in this work was achieved by using electrolyte containing 1 wt% of MWCNT. After the cross-linking process, the dimensional stability of the gel composite electrolyte was improved and the conversion efficiency of DSSC was only slightly affected, changing from 3.37% (before cross-linking) to 3.35%.

© 2012 Elsevier B.V. All rights reserved.

1. Introduction

Dye-sensitized solar cells (DSSC) have been under intense investigation since the first publication reported by O'Regan and Grätzel in 1991 [1]. The possibility to produce these solar cells at low cost and their relatively high energy conversion efficiency, reaching $10.3\% \pm 0.34\%$ (value for a 1 cm² cell) [2,3] make such devices promising alternatives for cheap electricity compared to the classical silicon-based photovoltaic panels [4]. The working principle of this device is relatively simple. First, dye molecules adsorbed on TiO₂ nanoparticles are excited by photons, followed by an ultrafast electron injection into the conduction band of the semiconductor oxide. Dye cations are regenerated by redox species (I⁻/I₃⁻ redox couple, for example) present in the electrolyte. Reduction of oxidized redox species is completed at the catalytic Pt layer of the counter electrode.

The electrolyte is an important component in determining the efficiency and durability of DSSC. A liquid electrolyte is usually composed of organic solvents employed to dissolve the redox couple [5–7]. However, liquid electrolytes have some shortcomings for long-term practical operation of DSSC due to leakage and solvent evaporation, which result in some difficulties for large scale production and market deployment of DSSC [8]. Efforts have been made in order to overcome these problems by replacing the liquid electrolyte by room temperature ionic liquids [9,10], inorganic hole transport materials [11–13], polymer electrolytes [14–18], or a mixture of carbon nanotubes with polymers, to give rise to composite materials [19].

Since their discovery by Iijima in 1991 [20], carbon nanotubes have received significant attention due to their dimensions and structure-sensitive properties. Basically, carbon nanotubes can be divided into two categories: single-wall carbon nanotubes (SWCNT) and multi-wall carbon nanotubes (MWCNT). This classification depends on the folding angle and the diameter; SWCNT can be metallic, insulating or semiconducting, whereas MWCNT are all conductive [21]. Several contributions report excellent electronic properties of carbon nanotubes for application as thin-film

* Corresponding author. Tel.: +55 19 3521 3029; fax: +55 19 3521 3023.
E-mail address: anafavia@iqm.unicamp.br (A.F. Nogueira).

transistors [22], diodes [23], chemical sensors [24] and more recently as the catalytic layer for counter electrodes in DSSC [25,26]. In addition, the presence of MWCNT may also improve the conductivity and mechanical properties of the electrolyte.

Yanagida and co-workers [27] investigated the effect of incorporating carbon nanotubes and different kinds of nanoparticles into the 1-ethyl-3-methylimidazolium bis(trifluoromethylsulfonyl)imide ionic liquid electrolyte. These authors observed a substantial increase in the viscosity and conductivity of the system in which carbon nanotubes were dispersed. The energy conversion efficiency of the DSSC assembled with that electrolyte containing 2 wt% MWCNT was 4.79% [27]. Ikeda and Miyasaka [28] have demonstrated the possibility of using SWCNT and ionic liquid in solid-state DSSC. By using this strategy, a conversion efficiency of 2.3% was achieved under simulated sunlight intensity of 23 mW cm^{-2} . Miyasaka and collaborators also reported solid-state DSSC using a conductive composite composed of polymer-loaded carbon black and ionic liquid [29]. A power conversion efficiency of 4.07% was then reported, demonstrating that a soft conductive material endowed with current rectifying ability is capable of generating a high photocurrent density by providing a good electric junction with the TiO_2 surface [29]. Thus, a promising alternative to enhance conductivity in the polymer electrolyte would be the addition of components into the polymer/salt system to give rise to a “composite gel electrolyte”.

We have demonstrated in our previous work the performance of DSSC assembled with a gel polymer electrolyte without the incorporation of CNT [30]. This electrolyte was composed of a poly(ethylene oxide) derivative, mixed with γ -butyrolactone (GBL), LiI and I_2 . The electrolyte containing 70% in weight of GBL and 20% of LiI provided the highest conductivity ($1.9 \times 10^{-3} \text{ S cm}^{-1}$) and, at the same time, the highest energy conversion efficiency (4.4% under illumination of 100 mW cm^{-2}) and dimensional stability compared to DSSC based on the other electrolyte compositions studied. Another alternative to further improve the mechanical properties of the polymer electrolyte is by means of the cross-linking process, which enables a significant enhancement in the dimensional stability of the whole electrolyte [31,32]. Nonetheless, the cross-linking process usually gives rise to poorer electrolyte conductivity, which is attributed to the slower motion of ions in the gel polymer matrix [33]. The addition of carbon nanotubes to the electrolyte composition provides means to overcome such drawback, mainly by enhancing electrolyte conductivity and, therefore, the performance of DSSC. The ability of polymer electrolytes containing carbon nanotubes to promote electron transfer reactions in many electrochemical systems has been reported in the literature [34–36], including dye-sensitized solar cells [37]. In this work, the role of carbon nanotubes in the polymer electrolyte for application in DSSC will be discussed. The addition of carbon nanotubes to the polymer electrolyte promoted a higher conductivity up to 1 wt% of MWCNT, but higher loadings provided poorer conductivity, probably due to carbon nanotube agglomeration and/or their interaction with Li^+ ions present in the electrolyte composition. The higher electrolyte viscosity, arising from the cross-linking process of the polymer electrolyte, brought about a smaller amount of polyiodide species, which is an interesting feature for DSSC application, since the presence of polyiodide species contributes to lower V_{oc} values due to high degree of charge recombination. Thus, in this paper, we report the preparation, characterization and application of a new cross-linked gel polymer electrolyte composed by the terpolymer poly(ethylene oxide-co-2-(2-methoxyethoxy) ethyl glycidyl ether-co-allyl glycidyl ether (P(EO/EM/AGE)), γ -butyrolactone (GBL), LiI and I_2 mixed with multi-wall carbon nanotubes (MWCNT) in dye-sensitized solar cells. The conductivities of the electrolytes as a function of carbon nanotubes content were analyzed. The samples were also investigated by Raman spectroscopy, thermal analysis

and diffuse reflectance measurements. Several DSSC were assembled with the new gel polymer electrolyte prepared with different amounts of MWCNT.

2. Experimental

2.1. Functionalization and characterization of multi-wall carbon nanotubes

MWCNT (CNT Co., Ltd., Seoul, Korea) were oxidized in a concentrated acid mixture of $\text{H}_2\text{SO}_4/\text{HNO}_3 = 3:1$ (Aldrich) (in volume) under ultrasonication for 24 h at 60°C to produce MWCNT containing carboxylic groups (and other polar groups), according to the procedure reported in literature [38–40]. The resulting solution was removed by filtration by using poly(tetrafluoroethylene) membranes. The solid was washed thoroughly with deionized water. Decantation was used to remove any remaining acid, followed by drying in an oven at 200°C . The insertion of carboxyl groups on the surface of carbon nanotubes increases their polarity, reactivity and contributes to a more effective interaction with the terpolymer, increasing dispersion into the polymer matrix [41].

Field emission scanning electron microscopy (FESEM) and high-resolution transmission electron microscopy (HRTEM) images were obtained using FEG-SEM JSC 6330F and HRTEM-JEM 3010 URP microscopes, respectively, at the Brazilian National Nanotechnology Laboratory (LNNano), Campinas, Brazil.

2.2. Preparation of gel polymer electrolytes containing MWCNT

The terpolymer poly(ethylene oxide-co-2-(2-methoxyethoxy) ethyl glycidyl ether-co-allyl glycidyl ether) P(EO/EM/AGE) was used as received from Daiso Co., Ltd. (Osaka, Japan) with a molar mass of $1 \times 10^6 \text{ g mol}^{-1}$, according to the supplier. The polymer samples were prepared by the dissolution of the terpolymer, LiI, I_2 and γ -butyrolactone (GBL) (Aldrich, 99%) in 15 mL of acetone. The P(EO/EM/AGE):GLB ratio was 0.1:0.9 (wt%) and the concentration of LiI and I_2 was kept constant at 20 wt% and at 2 wt%, respectively. After the preparation of the electrolyte, different amounts of functionalized MWCNT (0.5%, 1%, 1.25, 1.5%, and 3% (wt%)) were added to the polymer electrolyte composition.

2.3. Cross-linking procedure

Cross-linking was carried out by using benzoyl peroxide (Aldrich) as the initiator to the polymer solution, as described in the literature [42]. Peroxide was used in excess of the stoichiometric ratio in order to make sure all double bonds of the allyl glycidyl ether present at 1.7 wt% in the polymer structure would react. Reagents were weighted and then mixed. A volume of 10 mL of acetone was added to the mixture for complete dissolution of components. Electrolyte solutions were kept under stirring for 1 week before use. After evaporation of solvent to form films, it is necessary to maintain the systems at constant temperature (60°C) for 1 h.

2.4. Conductivity measurements

Conductivity measurements were evaluated as a function of MWCNT content. Electrolyte solutions were dropped onto stainless steel disks (area of 1.0 cm^2). A 0.05-mm-thick Teflon[®] spacer was used to prevent short-circuits and to maintain a controlled distance between the disks. In order to investigate the effect of cross-linking on the ionic conductivity, the samples were placed in an oven at 60°C for 1 h. After complete evaporation of solvent under air atmosphere for 50 h, samples were kept in a desiccator with P_2O_5 to remove humidity. The systems were sandwiched inside an MBraun

dry box (humidity < 10⁻⁴%, under an argon atmosphere) using a second stainless steel disk with the same area of the first and waited 72 h before measurements. Conductivity values were calculated from electrochemical impedance spectroscopy (EIS) data, using an Eco-Chemie Autolab PGSTAT 12 with a frequency resonance analyzer (FRA) module coupled to a computer, in the frequency range of 10 to 10⁵ Hz and an applied alternating current (AC) amplitude of 10 mV. The conductivity values were calculated from the bulk electrolyte resistance values arising from the complex impedance diagram.

2.5. Raman spectroscopy

The Raman spectra of MWCNT (before and after functionalization) and of cross-linked gel polymer electrolytes containing different amounts of MWCNT were measured in a Raman spectrometer, Micro-Raman Renishaw System 3000, equipped with a charge-coupled device (CCD) detector and an Olympus BTH 2 microscope. The excitation laser was set at 632.8 nm.

2.6. Diffuse reflectance measurements

The diffuse reflectance spectra of electrolyte samples were measured in a Varian spectrophotometer, model Cary 5G UV-VIS, NIR, with a diffuse reflectance accessory. Measurements were taken from 200 to 800 nm, using Teflon as a reference material for all samples. The electrolyte samples were sandwiched between two quartz plates by using Scotch[®] tape as spacer (60 μm). The following samples were analyzed: polymer electrolyte before cross-linking (no MWCNT), polymer electrolyte after cross-linking (no MWCNT) and polymer electrolyte after cross-linking containing 3% in weight of MWCNT.

2.7. Thermal characterization

Differential scanning calorimetry (DSC) curves of the gel polymer electrolytes prepared with different amounts of MWCNT were measured on a T.A. Instrument model 2100 coupled to a T.A. 2100 data analysis system. The average sample weight was within the range of 18–20 mg. All experiments were performed under a nitrogen flow rate of 100 mL min⁻¹. The samples were first heated at 100 °C for 5 min to eliminate thermal history. After cooling the samples to -100 °C at a rate of 10 °C min⁻¹, they were heated again to 100 °C at a rate of 10 °C min⁻¹. The DSC curves presented here are related to this second heating step.

2.8. Assembly and solar cells characterization

Solar cells were assembled with 0.25 cm² of active area. A TiO₂ suspension (Solaronix) was deposited by the doctor blading technique onto the FTO (fluorine-doped tin oxide) substrate (Hartford Glass Co., Inc., 8–12 Ω cm⁻²). The films were heated to 450 °C for 30 min, giving a layer of ~8 μm thickness as measured with a Taylor/Hobson Formtalysurf 50 profilometer. The electrodes were immersed in a 1.5 × 10⁻⁴ mol L⁻¹ solution of the complex [cis-bis(isothiocyanate) bis(2,2-bipyridyl)-4,4-dicarboxylate]ruthenium(II) bis-tetrabutylammonium (also known as N-719, Solaronix) in anhydrous ethanol for 20 h at room temperature. Afterwards, the electrodes were washed with ethanol and dried in air. The electrolyte deposition onto the TiO₂/dye photoelectrode was done inside a vacuum chamber using the method introduced by Caruso and co-workers [43]. Vacuum helps to ensure a better penetration of the polymer electrolyte inside the pores. Afterwards, photoelectrodes were heated to 60 °C during 1 h on a hot plate to remove acetone and to enable cross-linking in the presence of benzoyl peroxide. This step is crucial since the *in situ*

chemical cross-linking process takes place after the electrolyte has been infiltrated into the pores of the TiO₂ electrodes. Subsequently, Pt counter electrodes were then pressed onto the top of the gel electrolyte films.

J-V curves under illumination of 100 mW cm⁻² were measured under standard AM 1.5 condition by using a Xe (Hg) lamp as light source and filters. The polychromatic light intensity at the photoelectrode position was measured with a Newport Optical Power Meter model 1830-C.

3. Results and discussion

3.1. Morphological characterization and Raman spectroscopy of MWCNT

Fig. 1a and b shows scanning electron microscopy (FESEM) and high-resolution transmission electron microscopy (HRTEM) images of oxidized MWCNT, respectively. Fig. 1c presents the Raman spectra of MWCNT before and after functionalization that introduced carboxylic groups on the carbon nanotubes.

The FESEM image depicted in Fig. 1a shows randomly oriented MWCNT, and some of them are in the bundled form, as reported in literature [44]. However, smaller tube diameters were not present in large quantity. The same effect was also observed in the high-resolution transmission electron microscopy (HRTEM) image of Fig. 1b. Basically, a smaller tube diameter implies a higher curvature and strain of tube walls [45]. This effect is correlated with the chemical properties of MWCNT: smaller nanotubes are oxidized faster, while larger ones are less reactive and remain nearly unchanged [45,46].

Raman spectroscopy is a powerful tool for characterizing structural modifications such as defects on the surface of carbon nanotube samples after chemical treatments. Therefore, this technique was used to investigate the effect of acid treatment on the structure of carbon nanotubes. Fig. 1c shows the Raman spectra of MWCNT samples before and after acid treatment. They present typical Raman spectra featuring two principal characteristic peaks. The D-band at 1327 cm⁻¹ for MWCNT and 1338 cm⁻¹ for MWCNT-COOH corresponds to an A_{1g} mode due to local defects of the graphite crystal [47,48] and can also be related to the degree of defects or dangling bonds on the tube walls. The G-band at 1583 cm⁻¹ for MWCNT and 1595 cm⁻¹ for MWCNT-COOH is related to the graphitic E_{2g} symmetry of the interlayer mode, which reflects the structural integrity of the sp²-hybridized carbon atoms of the tubes [45,49]. Furthermore, a weak D'-band, attributed to a double-resonance Raman feature induced by disorder and defects [50], is observed at 1611 cm⁻¹ and 1616 cm⁻¹ for MWCNT and MWCNT-COOH, respectively.

The intensity ratio of the D and G band is a useful parameter to illustrate structural modification in MWCNT samples. The larger the I_D/I_G ratio is, the higher the modification degree of MWCNT. As can be seen in Fig. 1c, the I_D/I_G ratio observed in the MWCNT-COOH spectrum (I_D/I_G = 1.26) is higher than that observed in the MWCNT spectrum (I_D/I_G = 1.16). Furthermore, an upshift of the MWCNT-COOH spectrum is observed, which is related to a direct electron charge transfer process from nanotubes to acceptor pendant groups [51]. In light of this, it is clear that structural modification or defects originating from the addition of functional groups such as -COOH were achieved after acid treatment. Therefore, acid treatment has provided successful surface modification by adding -COOH groups (and, to a lesser extent, other functional groups), allowing solubility enhancement of MWCNT in the gel polymer electrolyte.

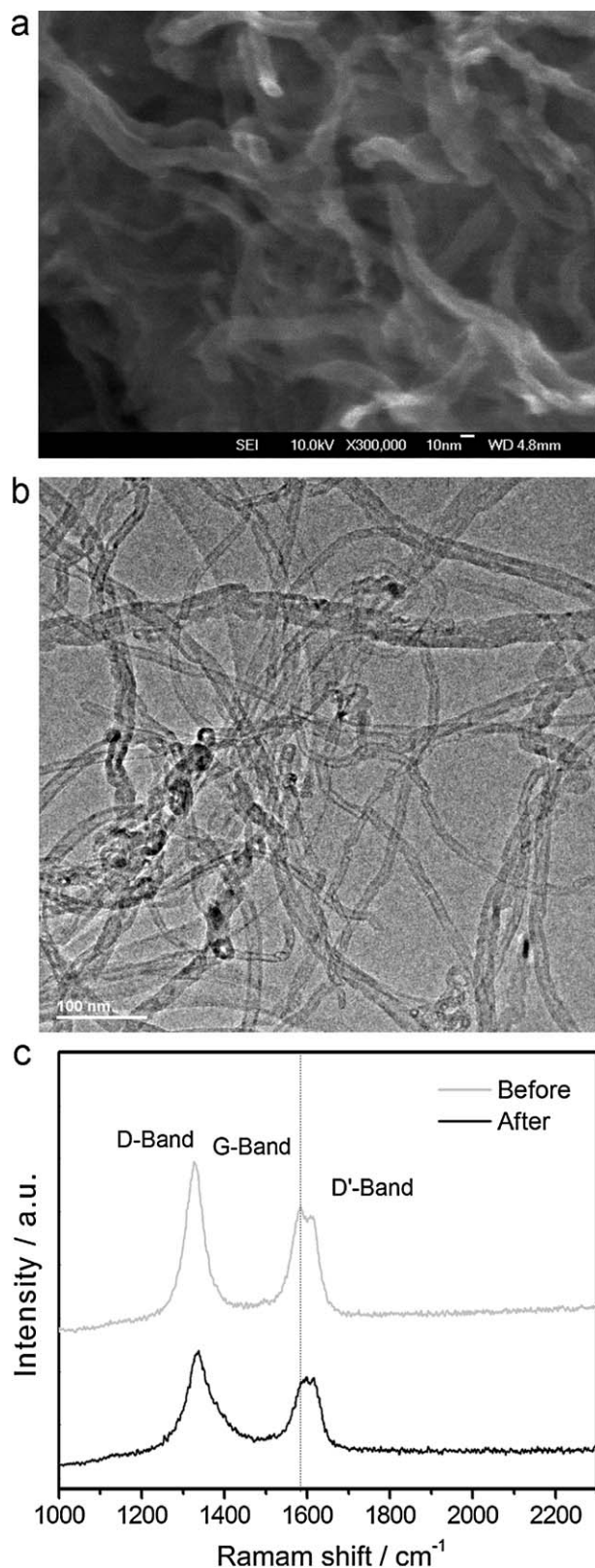


Fig. 1. (a) Scanning electron microscopy (FESEM) and (b) high-resolution transmission electron microscopy (HRTEM) images of MWCNT after oxidation and (c) Raman spectra of MWCNT before and after functionalization (laser excitation set at 632.8 nm).

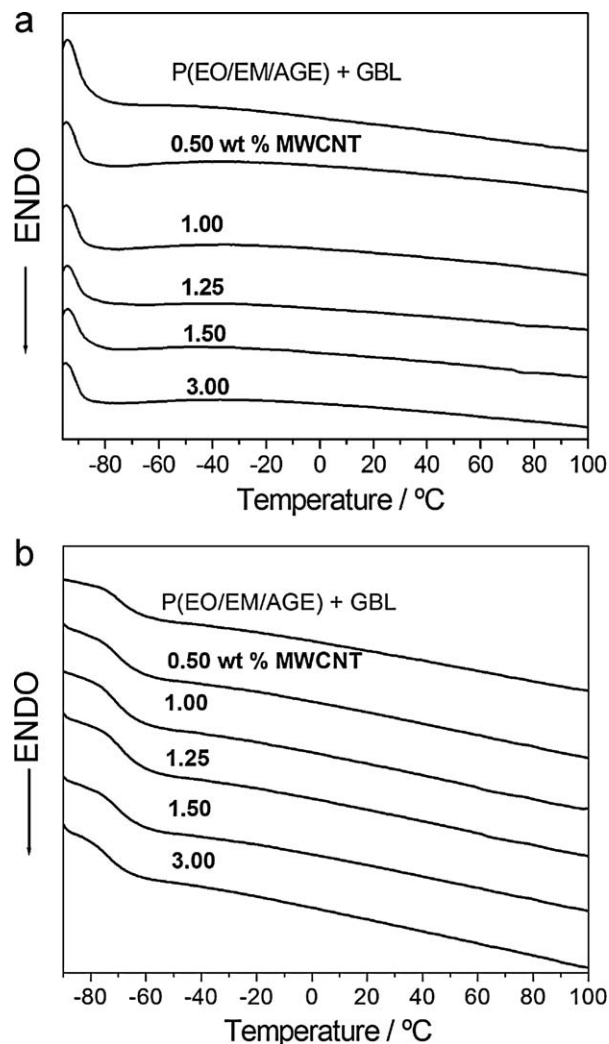


Fig. 2. DSC curves of composite gel polymer electrolyte prepared with different MWCNT concentrations: (a) before and (b) after cross-linking.

3.2. Thermal analysis of the composite gel polymer electrolyte

The thermal behavior of the composite gel polymer electrolyte (P(EO/EM/AGE)/GBL/MWCNT/LiI/L₂) was investigated. Fig. 2a shows the DSC curves of the composite gel polymer electrolyte prepared with different MWCNT contents before cross-linking and Fig. 2b presents the DSC curves of the composite gel polymer electrolyte prepared with different amounts of MWCNT after the cross-linking process. The amount of copolymer, GBL, salt and iodine were kept constant. As described in Section 2, only the content of functionalized MWCNT was varied in the samples (0.5, 1, 1.25, 1.5 and 3 wt%).

As observed in Fig. 2, crystalline peaks were not identified for any of the samples, indicating that the composite polymer electrolyte investigated in this work is predominantly amorphous. This is an important property, since ionic motion in gel polymer electrolytes also depends on solvation–desolvation processes along the polymer chains, which occur with a large contribution from the amorphous polymer phase [52]. Ionic motion is strictly correlated with the segmental motion of the polymer chains. Therefore, glass transition temperatures below -65°C are important for application as photoelectrochemical devices, since at room temperature the polymer already has some segmental mobility, which contributes to the effective conduction of ions in the electrolyte. Additional information on the thermal properties of the electrolyte may be

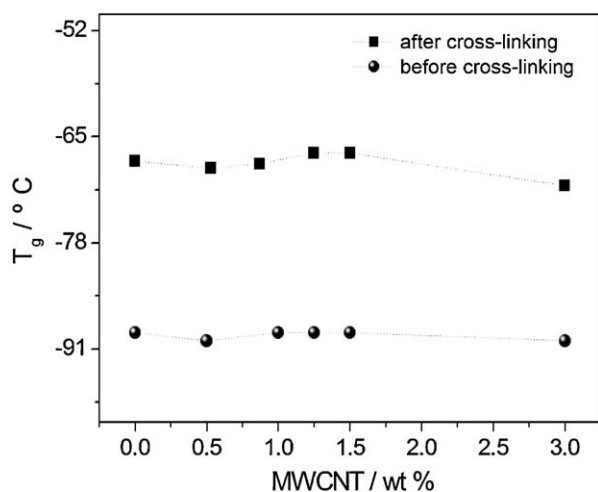


Fig. 3. Dependence of glass transition temperature (T_g) on MWCNT concentration and on the cross-linking process.

gathered from the analysis of T_g as a function of temperature, as shown from data in Fig. 3.

Fig. 3 presents the T_g values estimated from DSC data for the composite gel polymer electrolytes prepared as a function of MWCNT concentration, before and after cross-linking for the sake of comparison.

Two different behaviors are observed in Fig. 3. First, after cross-linking, an increase of T_g was observed for all MWCNT concentrations. This result suggested that cross-linking reduces the local motion of the polymer segment through the formation of covalent bonds between polymer chains, causing an increase of T_g values. The same effect has already been reported by De Paoli and co-workers [42] for the solid electrolyte prepared with poly (ethyleneoxide-co-2-(2-methoxyethoxy) ethylglycidyl ether-co-allylglycidyl ether and lithium perchlorate. Second, according to the behavior clearly observed from data shown in Fig. 3, there was no relevant change on T_g for the system containing carbon nanotubes in the electrolyte. This result provides evidence that carbon nanotubes modified with polar groups would interact only at the interface region with the P(EO/EM/AGE) polymer matrix, not impairing the mobility of the polymer chains.

3.3. Conductivity measurements

Fig. 4 shows the conductivities calculated using data from impedance spectroscopy (data not shown) at 25 °C for P(EO/EM/AGE)/GBL/MWCNT/LiI/I₂ electrolyte containing different MWCNT concentrations, before and after cross-linking. The inset at the left-hand side of Fig. 4 shows a digital picture of the composite gel polymer electrolyte before (I) and after (II) cross-linking. As observed in the photography, for the gel polymer electrolyte samples, no fluidity is observed at room temperature, due to the formation of three-dimensional polymer network. This is an important feature for application as an electrolyte in DSSC, since it would help to minimize solvent leakage problems. The inset at the right-hand side of Fig. 4 presents the composite gel electrolyte containing different amounts of carbon nanotubes after cross-linking. The composite gel polymer electrolyte samples get darker as the amount of carbon nanotubes increases.

The conductivity of gel electrolyte samples without MWCNT was $7.9 \times 10^{-4} \text{ S cm}^{-1}$, which decreased to $5.5 \times 10^{-4} \text{ S cm}^{-1}$ after the cross-linking process. As discussed previously, the mobility in the polymer electrolyte depends on the dissolution of ions in the polymer matrix, which is facilitated by the segment mobility of the polymer chains [53]. Thus, the reduction of segment mobility of the

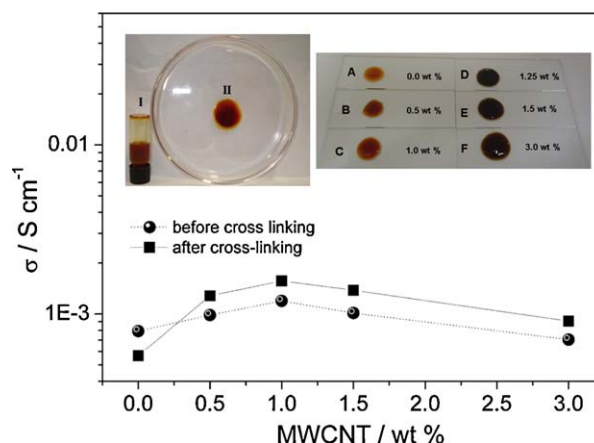


Fig. 4. Conductivity of composite gel polymer electrolytes P(EO/EM/AGE)/GBL/MWCNT/LiI/I₂ prepared with different amounts of MWCNT, before and after cross-linking. The left-hand inset is a digital picture of the gel polymer electrolyte before (I) and after (II) cross-linking. The right-hand side inset shows a digital photograph of the cross-linked gel polymer electrolyte samples prepared with different contents of carbon nanotubes after the cross linking process: (A) without MWCNT, (B) 0.5 wt%, (C) 1.0 wt%, (D) 1.25 wt%, (E) 1.5 wt% and (F) 3 wt% of MWCNT.

polymer chains by the cross-linking process caused a decrease in the ionic conductivity of the electrolyte, which is reflected by the drop in overall conductivity [18]. Similar results were described in literature for electrolytes prepared with poly (ethylene imine) and poly (ethylene glycol) containing different amounts of cross-linking agent [54].

Before discussing the conductivity behavior for composite electrolytes containing MWCNT, it is important to mention that the overall conductivity of the P(EO/EM/AGE)/GBL/MWCNT/LiI/I₂ system is composed of ionic conductivity, arising from dissociated salts in the system, and also of electronic conductivity stemming from MWCNT in the electrolyte composition [41,55]. However, the separation of ionic and electronic contributions to the overall polymer electrolyte conductivity is not straightforward. Such a separation could be performed by means of AC impedance spectroscopy measurements [56]. The Nyquist plots of the gel polymer electrolyte sandwiched between two blocking electrodes did not exhibit the typical semicircle at the high frequency region, normally observed when measuring the impedance of a classical polymer electrolyte (polymer and salt only) [57,58], which makes it difficult for separating these electrochemical processes in this study.

The addition of MWCNT into the electrolyte provides an interesting behavior. For both systems, before and after cross-linking, a similar behavior is observed, that is, a higher electrolyte conductivity as the MWCNT content increases. The maximum electrolyte conductivity for both systems (before and after cross-linking) was reached for the electrolyte composition containing 1 wt% MWCNT and after that the electrolyte conductivity slightly decreased up to the maximum MWCNT concentration investigated in this work (3 wt%).

The higher electrolyte conductivity with the addition of small amounts of MWCNT (up to 1 wt%) is, probably, a contribution from the electronic conductivity of the system provided by the presence of MWCNT in the electrolyte composition. Previous reports have shown a significant increase in the electrical conductivity of polymer matrices with the incorporation of small amounts of carbon nanotubes in the system [41,59].

As shown in Fig. 4, the electrolyte conductivity drops slightly after the addition of more than 1 wt% of MWCNT. This decrease in electrolyte conductivity for MWCNT concentrations higher than 1 wt% may be explained by the possible interaction of polar groups

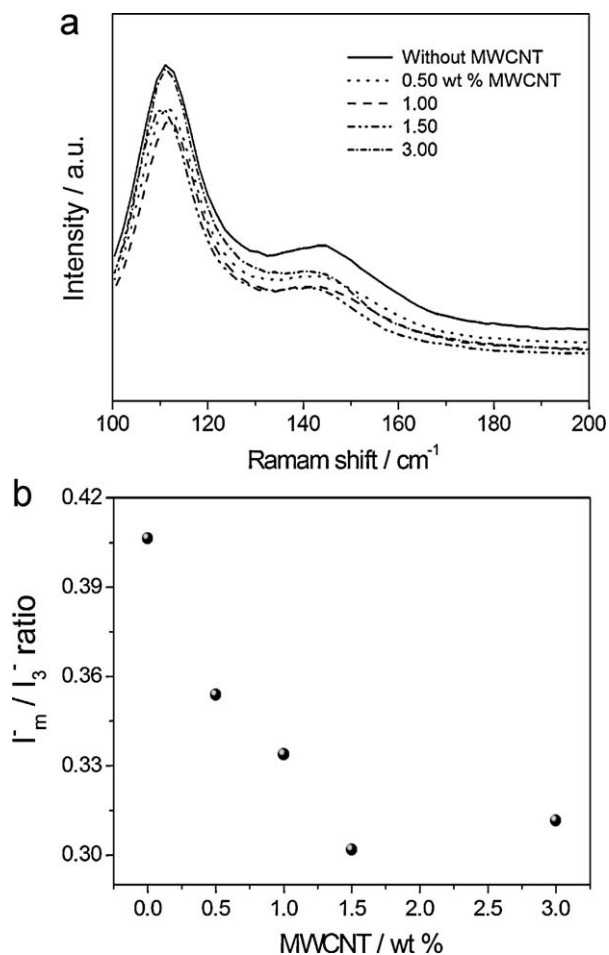


Fig. 5. (a) Raman spectra as a function of MWCNT concentration for the cross-linked polymer electrolyte, laser excitation wavelength set at 632.8 nm; (b) ratio of polyiodides (I_m^-) and I_3^- (I_m^-/I_3^-) as a function of MWCNT for the gel polymer electrolyte.

present on the MWCNT surface with Li^+ ions in the electrolyte composition. As reported earlier [38,39], the functionalization of MWCNT provides carboxylic and other polar groups on the surface of the carbon nanotubes, which are important for improving the interaction with the also polar P(EO/EM/AGE) matrix. However, the higher concentration of functionalized MWCNT in the system (higher than 1 wt%) might give rise to a more effective interaction between Li^+ cations and polar groups attached to MWCNT, which decreases to some extent the ion mobility in the electrolyte. This effect would decrease the ionic conductivity of the electrolyte and, consequently, the overall conductivity of the system. The presence of carbon nanotube agglomerates cannot be ruled out for MWCNT loadings higher than 1 wt%, which could also decrease conductivity due to a more difficult ionic motion in the electrolyte [55].

3.4. Raman spectroscopy of composite gel polymer electrolyte

Fig. 5a shows the Raman spectra of the composite gel polymer electrolytes P(EO/EM/AGE)/GBL/MWCNT/LiI/I₂ as a function of MWCNT concentration after the cross-linking process. As observed in this Fig., all samples showed a band around 110 cm^{-1} , which can be assigned to the symmetric stretch of I_3^- species [60,61]. Another band for all composite electrolyte samples related with the vibration mode of higher polyiodide species was observed at $\sim 142\text{--}145\text{ }cm^{-1}$ [62,63]. Polyiodide species (I_m^-) may contribute to electrical conduction into the electrolyte through Grothuss-type

Table 1

Electrical parameters for DSSC based on composite gel polymer electrolytes containing different amounts of MWCNT, before and after the cross-linking process.

MWCNT (wt%)	J_{sc} ($mA\text{ }cm^{-2}$)	V_{oc} (V)	FF	η (%)
Before cross-linking				
0.0	6.20	0.67	0.57	2.39
0.5	7.53	0.70	0.61	3.22
1.0	7.93	0.69	0.61	3.37
1.5	7.33	0.71	0.63	3.30
3.0	6.70	0.66	0.58	2.59
After cross-linking				
0.0	5.63	0.65	0.61	2.23
0.5	7.88	0.68	0.62	3.34
1.0	8.74	0.67	0.57	3.35
1.5	6.67	0.66	0.57	2.50
3.0	5.79	0.63	0.59	2.15

charge transfer. In the Grothuss-type charge transfer mechanism, electron hopping and the polyiodide bond exchange are coupled, contributing to the effective conductance of the polymer electrolyte [62].

The effect of MWCNT concentration on polyiodide formation in the electrolyte was investigated by analyzing the intensity ratio between polyiodide (I_m^-) and triiodide (I_3^-) species, as shown in Fig. 5b. The I_m^-/I_3^- ratio was calculated from the intensities of the peaks at 110 and 142 cm^{-1} . We can observe a decrease in the I_m^-/I_3^- ratio with the addition of MWCNT into the electrolyte (Fig. 5b). The generation of less polyiodides with a higher concentration of MWCNT suggests that the formation of this ionic species is favored by the low viscosity of the electrolyte. We have already observed this effect in a previous work with the increase in viscosity of the system [30]. The addition of MWCNT into the gel polymer electrolyte causes an increase in viscosity due to the interaction between carbon nanotubes and polymer chains. The higher the viscosity of the system, the poorer would be the collision of ionic species (I^-/I_3^-), giving rise to a smaller generation of polyiodides [30], as evidenced in Fig. 5b. Therefore, the higher viscosity enabled a lower concentration of the less-conducting polyiodide species and, consequently, a more conducting polymer electrolyte after the cross-linking process, according to Fig. 4. In our previous work [30], theoretical calculations indicated that polyiodide species are a better electron acceptor than tri-iodide due more delocalized charges, which makes the reaction with electrons more favorable due to less electron repulsion [30]. Thus, the decrease of the I_m^-/I_3^- ratio with higher MWCNT content probably contributes to reduce charge recombination losses in DSSC. This effect will be discussed further.

3.5. DSSC based on the composite gel polymer electrolyte

The J - V curves of the DSSC based on the gel polymer electrolytes at different MWCNT loadings are shown in Fig. 6 (a) before and (b) after the cross-linking process. The inset in Fig. 6 shows the dark current of the devices. The electrical parameters of the DSSC are summarized in Table 1.

The photovoltaic performance of the solar cells was influenced by the cross-linking process. As shown in Table 1, a decrease in short-circuit current density (J_{sc}), from 6.20 $mA\text{ }cm^{-2}$ to 5.63 $mA\text{ }cm^{-2}$, is observed after the cross-linking process when compared to DSSC based on the electrolyte composition without cross-linking. This effect is due to an increase in the resistance for ion migration (system hardening) caused by the formation of three-dimensional networks after cross-linking, which results in a decrease of photocurrent, as already reported in literature [64].

The addition of 1% in weight of MWCNT to the electrolyte composition without cross-linking improved the overall energy conversion efficiency from 2.39 to 3.37%. In this work, all the studied MWCNT loadings improved the conversion efficiency (η)

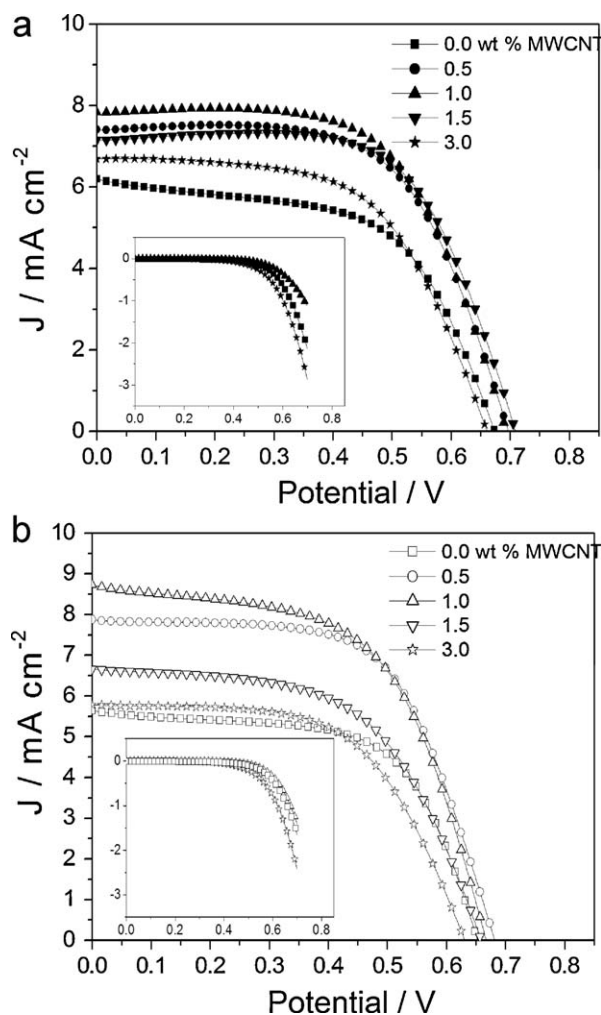


Fig. 6. J - V characteristics under illumination of 100 mW cm^{-2} for DSSC assembled with composite gel polymer electrolytes at different MWCNT loadings (0.5%, 1%, 1.5%, and 3 wt%) (a) before and (b) after cross-linking. Active cell area: 0.25 cm^2 , TiO_2 film thickness: $8 \mu\text{m}$. The insets in figure present the dark current curves.

compared to the same electrolyte without MWCNT. The higher conductivity of the electrolyte without cross-linking with 1 wt% of MWCNT, as shown in Fig. 4, can explain the maximum performance achieved for this group of electrolyte compositions.

The addition of MWCNT improved the overall conductivity of the gel polymer electrolyte even after cross-linking (Fig. 4). The enhanced charge transport properties of the cross-linked polymer electrolyte after the addition of MWCNT was also evaluated in DSSC. In Fig. 6 it is possible to observe that the addition of 1 wt% MWCNT to the cross-linked polymer electrolyte provided a higher performance when compared to the DSSC based on the cross-linked polymer electrolyte without MWCNT. The higher J_{sc} might be associated to enhanced charge transport properties of the polymer electrolyte, which functions as a mixed conductor, *i.e.*, ionic and electronic conductivities. However, the addition of 3 wt% of MWCNT to the cross-linked polymer electrolyte showed a decrease in J_{sc} and also in V_{oc} .

The drop in V_{oc} may be explained, at least in part, by the combination of two main recombination processes: electrons photoinjected into the TiO_2 conduction band/trap states might recombine with dye cations (Eq. (1)) and/or with electrolyte species (Eq. (2)) [30,65]:

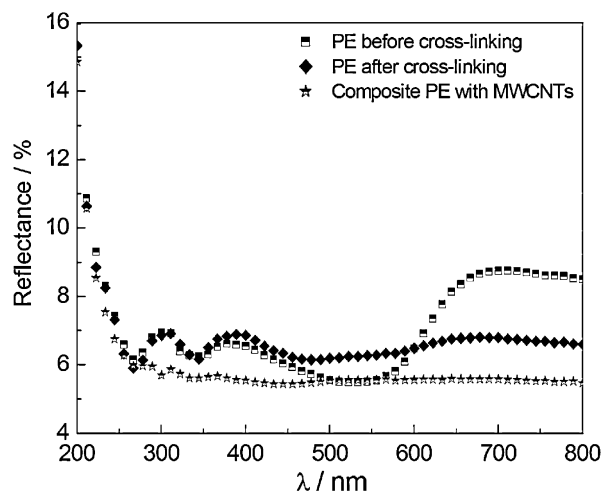


Fig. 7. Diffuse reflectance spectra of polymer electrolyte (PE) samples before and after cross-linking and composite electrolyte (containing 3 wt% MWCNT) after the cross-linking process.



Polyiodide species are responsible for increasing recombination losses [30]. According to the data shown in Fig. 5b, a decrease in polyiodide formation is observed due to the addition of MWCNT to the electrolyte composition. Therefore, it would be expected that V_{oc} would increase after the addition of MWCNT to the electrolyte composition. In fact, the incorporation of MWCNT up to 1.5 wt% promotes an increase in V_{oc} for devices in both cases (before and after the cross-linking process). Above this concentration, the opposite behavior was observed, *i.e.*, V_{oc} was lower for higher MWCNT concentrations (3 wt%). The poorer electrolyte conductivity for MWCNT loadings higher than 3 wt% would favor charge recombination losses arising from electrons in the TiO_2 conduction band/trap states and electrolyte acceptors, this way decreasing V_{oc} [30]. Some evidence for this behavior may be provided by J - V curves measured in the dark (Fig. 6a and b, insets), since DSSC based on the composite electrolyte containing 3 wt% of MWCNT exhibits higher dark current values.

The smaller J_{sc} achieved by increasing the amount of MWCNT beyond 1 wt% might be associated with the lower conductivity of the polymer electrolyte (Fig. 4) and to a poorer transmittance of the electrolyte in the visible range that can preclude light absorption (Fig. 7). Thus, the low transmittance of the composite electrolyte with MWCNT loadings higher than 1 wt% (Fig. 7) might impair light harvesting properties of the photoelectrode, since the light that was not absorbed by the sensitized TiO_2 electrode could not be reflected back at the mirror-like Pt counter electrode [66].

The addition of 1 wt% MWCNT to the polymer electrolyte composition provided the maximum performance in this work for both electrolyte systems: without or with cross-linking. It is important to note that the cross-linking process, along with MWCNT in the electrolyte composition, improved the dimensional stability of the electrolyte. This is an important requirement for quasi-solid state DSSC. Therefore, it was possible to increase the dimensional stability of the electrolyte without impairing the performance of the DSSC, when compared with the results of non-cross-linked polymer electrolyte with MWCNT.

4. Conclusions

The gel composite polymer electrolytes prepared with poly(ethylene oxide-*co*-2-(2-methoxyethoxy) ethyl glycidyl ether-*co*-allyl glycidyl ether), γ -butyrolactone, LiI , I_2 and functionalized

multi-wall carbon nanotubes (MWCNT) were investigated and applied in dye-sensitized solar cells (DSSC). Incorporation of MWCNT into the cross-linked electrolyte promoted improvements in the conductivity and a decrease in the polyiodide species, as confirmed by Raman spectroscopy measurements. The best performance was achieved for solar cells assembled with electrolyte containing 1 wt% MWCNT, with a conversion efficiency of 3.37%. After cross-linking, the dimensional stability of the gel composite electrolyte was improved while the efficiency of the DSSC was only slightly affected, changing from 3.37% to 3.35%.

Acknowledgments

The authors acknowledge Grupo Rede de Distribuição de Energia (fellowship Funcamp 6295), FAPESP (fellowships 2011/080304-6, 08/51001-9 and 08/53059-4), CNPq and Renami for financial support, Daiso Co. Ltd. Osaka (Japan) for kindly providing the copolymer and Prof. Carol H. Collins for English revision. We also acknowledge Prof. Victor Baranauskas (Electrical Engineer/UNICAMP) for the Raman facility and the Brazilian National Nanotechnology Laboratory (LNNano) for technical support.

References

- [1] B. O'Regan, M. Grätzel, *Nature* 353 (1991) 737.
- [2] M.A. Green, K. Emery, Y. Hishikawa, W. Warta, *Prog. Photovoltaics* 19 (2011) 84.
- [3] P.M. Peter, *J. Phys. Chem. Lett.* 2 (2011) 1861.
- [4] C. Longo, A.F. Nogueira, M.-A. De Paoli, H. Cachet, *J. Phys. Chem. B* 106 (2002) 5925.
- [5] M. Grätzel, *C. R. Chim.* 9 (2006) 578.
- [6] L.C.P. Almeida, A.D. Gonçalves, J.E. Benedetti, P.C.M.L. Miranda, L.C. Passoni, A.F. Nogueira, *J. Mater. Sci.* 45 (2010) 5054.
- [7] M. Grätzel, *J. Photochem. Photobiol. A* 3 (2004) 164.
- [8] B.I. Ito, J.N. Freitas, M.-A. De Paoli, A.F. Nogueira, *J. Braz. Chem. Soc.* 19 (2008).
- [9] P. Wang, S.M. Zakeeruddin, J.E. Moser, R.H. Baker, M. Grätzel, *J. Am. Chem. Soc.* 126 (2004) 7124.
- [10] S. Ito, S.M. Zakeeruddin, P. Comte, P. Liska, D. Kuang, M. Grätzel, *Nat. Photonics* 2 (2008) 693.
- [11] J. Bandara, H. Weerasinghe, *Sol. Energy Mater. Sol. Cells* 85 (2005) 385.
- [12] G.K.R. Senadeera, T. Kitamura, Y. Wada, S. Yanagida, *J. Photochem. Photobiol. A* 184 (2006) 234.
- [13] J.E. Kroeze, N. Hirata, L.S. Mende, C. Orizu, S.D. Ogier, K. Carr, M. Grätzel, *J.R. Durrant, Adv. Funct. Mater.* 16 (2006) 1832.
- [14] T. Kato, A. Okazaki, S. Hayase, *J. Photochem. Photobiol. A* 179 (2006) 42.
- [15] J.E. Benedetti, M.A. De Paoli, A.F. Nogueira, *Chem. Commun.* 9 (2008) 1121.
- [16] J.N. Freitas, C. Longo, A.F. Nogueira, M.-A. De Paoli, *Sol. Energy Mater. Sol. Cells* 92 (2008) 1110.
- [17] J. Wu, Z. Lan, J. Lin, M. Huang, S. Hao, T. Sato, S. Yin, *Adv. Mater.* 19 (2007) 4006.
- [18] J.N. Freitas, A.F. Nogueira, M.-A. De Paoli, *J. Mater. Chem.* 19 (2009) 5279.
- [19] X.H. Zhang, S.M. Wang, Z.X. Xu, J. Wu, L. Xin, *J. Photochem. Photobiol. A* 198 (2008) 288.
- [20] S. Iijima, *Nature* 354 (1991) 56.
- [21] M. Paradise, T. Goswami, *Mater. Des.* 28 (2007) 1477.
- [22] M. Meitl, Y. Zhou, A. Gaur, S. Jeon, M. Usrey, M. Strano, J. Rogers, *Nano Lett.* 4 (2004) 1643.
- [23] Y. Zhou, A. Gaur, S. Hur, C. Kocabas, M.A. Meitl, M. Shim, J. Rogers, *Nano Lett.* 4 (2004) 2031.
- [24] J. Abraham, B. Philip, A. Witchurch, V. Varadan, C. Reddy, *Smart Mater. Struct.* 13 (2004) 1045.
- [25] S. Hwang, J. Moon, S. Lee, D.H. Kim, D. Lee, W. Choi, M. Jeon, *Electron. Lett.* 43 (2007) 1455.
- [26] J.E. Trancik, S.C. Barton, J. Hone, *Nano Lett.* 8 (2008) 982.
- [27] H. Usui, H. Matsui, N. Tanabe, S. Yanagida, *J. Photochem. Photobiol. A* 164 (2004) 97.
- [28] N. Ikeda, T. Miyasaka, *Chem. Lett.* 36 (2007) 466.
- [29] N. Ikeda, K. Teshima, T. Miyasaka, *Chem. Commun.* (2006) 1733.
- [30] J.E. Benedetti, A.D. Gonçalves, A.L.B. Formiga, M.-A. De Paoli, X. Li, J.R. Durrant, A.F. Nogueira, *J. Power Sources* 195 (2010) 1246.
- [31] S. Oh, D.W. Kim, C. Lee, M.-H. Lee, Y. Kang, *Electrochim. Acta* 57 (2011) 46.
- [32] Y. Wang, *Sol. Energy Mater. Sol. Cells* 93 (2009) 1167.
- [33] M.S. Akhtar, Z.Y. Li, D.M. Park, D.W. Oh, D.-H. Kwak, O.-B. Yang, *Sol. Energy Mater. Sol. Cells* 91 (2007) 1892.
- [34] K.A. Emery, C.R. Osterwald, H. Aharoni, *Solid-State Electron.* 30 (1987) 213.
- [35] M.S. Akhtar, J.-G. Park, H.-C. Lee, S.-K. Lee, O.-B. Yang, *Electrochim. Acta* 55 (2010) 2418.
- [36] L. Zhang, W. Zhou, L. Wang, H. Fu, *Sci. Adv. Mater.* 1 (2009) 182.
- [37] M.S. Akhtar, Z.Y. Li, D.M. Park, D.W. Oh, D.-H. Kwak, O.B. Yang, *Electrochim. Acta* 56 (2011) 9973.
- [38] X. Nan, Z. Gu, Z. Liu, *J. Colloid Interface Sci.* 245 (2002) 311.
- [39] J. Liu, A.G. Rinzler, H. Dai, J.H. Hafner, R.K. Bradley, P.J. Boul, A. Lu, T. Iverson, K. Shelimov, C.B. Huffman, F.R. Macias, D.T. Colbert, R.E. Smalley, *Science* 280 (1998) 1253.
- [40] Z. Liu, Z. Shen, T. Zhu, S. Hou, L. Ying, Z. Shi, Z. Gu, *Langmuir* 16 (2000) 3569.
- [41] L.G. Pedroni, M.A. Soto-Oviedo, J.M. Rosolen, M.I. Felisberti, A.F. Nogueira, *J. Appl. Polym. Sci.* 112 (2009) 3241.
- [42] A.T. Cruz, G.G. Silva, P.P. De Souza, T. Matencio, J.M. Pernaut, M.-A. De Paoli, *Solid State Ionics* 159 (2003) 301.
- [43] H.W. Han, U. Bach, Y.B. Cheng, R.A. Caruso, *Appl. Phys. Lett.* 90 (2007) 213510.
- [44] S.C. Canobre, D. Almeida, C.P. Fonseca, S. Neves, *Electrochim. Acta* 54 (2009) 6383.
- [45] I.D. Rosca, F. Watari, M. Uo, T. Akasaka, *Carbon* 43 (2005) 3124.
- [46] N. Yao, V. Lordi, S.X.C. Ma, E. Dujardin, A. Krishnan, M.M.J. Treacy, T.W. Ebbesen, *J. Mater. Res.* 13 (1998) 2432.
- [47] M. Yudasaka, R. Kikuchi, T. Mastui, H. Kamo, Y. Ohki, S. Yoshimura, E. Ota, S. Yoshimura, *Appl. Phys. Lett.* 64 (1994) 842.
- [48] M. Yudasaka, L. Dai, S. Huang, A.W.H. Mau, Z.L. Wang, *Chem. Phys. Lett.* 316 (2000) 349.
- [49] H. Zhang, C.H. Sun, F. Li, H.X. Li, H.M. Cheng, *J. Phys. Chem. B* 110 (2006) 9477.
- [50] K. Behler, S. Osswald, H. Ye, S. Dimovski, Y. Gogotsi, *J. Nanopart. Res.* 8 (2006) 615.
- [51] A.M. Rao, S. Bandow, E. Richter, P.C. Eklund, *Thin Solid Films* 331 (1998) 141.
- [52] A.F. Nogueira, C. Longo, M.-A. De Paoli, *Coord. Chem. Rev.* 248 (2004) 1455.
- [53] P. Santhosh, T. Vasudevan, A. Gopalan, K.P. Lee, *J. Power Sources* 160 (2006) 609.
- [54] S.J. Lim, Y.S. Kang, D.W. Kim, *Electrochem. Commun.* 12 (2010) 1037.
- [55] A. Chinduang, P. Duangkaew, S. Pratontep, G. Tumcharen, *Adv. Mater. Res.* (93–94) (2010) 31.
- [56] X. Guo, J. Fleig, J. Maier, *J. Electrochem. Soc.* 148 (2001) J50.
- [57] T.T. Cezare, S. Neves, *J. Power Sources* 112 (2002) 395.
- [58] C.P. Fonseca, S. Neves, *J. Power Sources* 159 (2006) 712.
- [59] C. Luo, X. Zuo, L. Wang, E. Wang, S. Song, J. Wang, J. Wang, C. Fan, Y. Cao, *Nano Lett.* 8 (2008) 4454.
- [60] L. Andrews, E.S. Prochaska, A. Loewenschuss, *Inorg. Chem.* 19 (1980) 463.
- [61] M.A. Tadayoni, P. Gao, M.J. Weaver, *J. Electroanal. Chem.* 198 (1986) 125.
- [62] W. Kubo, K. Murakoshi, K. Kitamura, S. Yoshida, M. Haruki, H. Hanabusa, H. Shirai, Y. Wada, S. Yanagida, *J. Phys. Chem. B* 105 (2001) 12809.
- [63] I. Jerman, V. Jovanovski, A.S. Vuk, S.B. Hocevar, M. Gaberscek, A. Jesih, B. Orel, *Electrochim. Acta* 53 (2008) 2281.
- [64] S.J. Lim, Y.S. Kang, D.W. Kim, *Electrochem. Commun.* 12 (2010) 1037.
- [65] J.N. Freitas, A.S. Gonçalves, J.R. Durrant, M.-A. De Paoli, A.F. Nogueira, *Electrochim. Acta* 53 (2008) 7166.
- [66] M.K. Nazeeruddin, R.H. Baker, M. Grätzel, *J. Phys. Chem. B* 107 (2003) 8981.